Precision of Silicon Oxynitride Refractive-Index Profile Retrieval Using Optical Characterization

V. Kanclíř*, J. Václavík and K. Žídek

Regional Centre for Special Optics and Optoelectronic Systems (TOPTEC), Institute of Plasma Physics, Academy of Sciences of the Czech Republic, Za Slovankou 1782/3, 182 00 Prague 8, Czech Republic

Received: 04.05.2021 & Accepted: 23.08.2021

Doi: 10.12693/APhysPolA.140.215 *e-mail: kanclir@ipp.cas.cz

Layers with a gradient refractive-index profile are an attractive alternative to conventional homogeneous stack coatings. However, the optical characterization and monitoring of the graded refractive-index profile is a complex issue that has usually been solved with a simplified model of mixed materials. Although such an approach provides a solution to the problem, the precision, which can be expected from optical characterization of the refractive-index gradient, remains unclear. In this work, we study optical characterization of SiO_xN_y layers deposited via reactive dual ion beam sputtering. To characterize the deposited layers, we use several methods including reflectance and transmittance spectra at a broad range of incident angles together with spectral ellipsometry. All the data were simultaneously fitted with a general profile of the refractive index. The expected profile used in our fit was based on the characterization of SiO_xN_y layers with a varying stoichiometry. By altering the profile, we discussed the sensitivity of alternation on the fit quality and we studied the ambiguity of the merit-function minimization. We demonstrate that while the scanning of particular parameters of the profile can be seemingly very precise, we obtain a very good agreement between the experimental data and the model for a broad range of gradient shapes. Our calculation shows that the refractive-index value on the major part of the profile can differ as much as 0.02 from the mean value.

topics: gradient refractive-index layers, silicon oxynitride, dual ion beam sputtering, precision of optical characterization

1. Introduction

Optical coatings consisting of a stack of thin dielectric layers are extensively employed to improve the characteristics of optical elements, most commonly by adjusting their reflectance and transmittance. The desired optical response is typically attained by a deposition of alternating materials with a low and a high refractive index. Thicknesses of the layers of each of the materials determine the resulting properties of the stack. For several decades, an alternative approach has also been employed, where a refractive index within the coating is changing gradually. This approach features several advantages, such as the absence of interfaces between the high and the low refractive-index films which can improve the laser-induced damage threshold [1, 2]. In the case of rugate filters, which have a graded refractive-index profile, their stop bands are not surrounded by sidelobes and produce no harmonic stop bands. This is unlike a quarter-wave stack of homogeneous layers [3].

A material commonly used in the deposition of gradient layers is silicon oxynitrid (SiO_xN_y). Its advantages are the transparency in VIS and NIR spectra together with a wide range of the refractive index varying at the wavelength of 500 nm between 2.063 for Si_3N_4 [4] and 1.468 for SiO_2 [5]. A variety of techniques can be used for SiO_xN_y deposition, including the plasma enhanced chemical vapour deposition [6], ion assisted deposition [7], magnetron sputtering [8], or dual ion beam sputtering (DIBS) [9–12].

In order to attain a desired optical response, it is necessary to control and measure the refractive-index gradient. Two non-destructive methods are used for characterization: the spectral ellipsometry (SE) and the spectrophotometry, i.e., reflectance (R) and transmittance (T) measurements. The mentioned methods are indirect, thus a proper model is required to retrieve the refractive and extinction index. A typical problem appearing is the ambiguity of solutions, which arises even for the standard layers. The problem can be partly resolved by using the measurements of SE, T and R, taken at several angles [13, 14].

The characterization of the graded-index films is an even more complex problem as it is necessary to characterize the gradually varying profile. This is typically solved by dividing the layer into several homogeneous sublayers, where their number is high enough to ensure that the thickness of the sublayers is thinner than a quarter of the smallest wavelength [15]. A number of groups have already applied this approach either to the SE data [6, 7, 15–17], or to both the SE and spectrophotometric data [12, 13]. Most of the groups used the effective medium approximation (EMA) developed by Bruggeman [18] to model the refractive-index profile. The profile is obtained then from the knowledge of the relative volume fraction between SiO_2 and Si_3N_4. This method, however, strongly depends on the accuracy of outer indices and on the accuracy of the volume ratio. Since EMA can be a model for composite materials, thus it is not physical for SiO_xN_y, although it is functioning as a reasonable approximation [19]. A very different approach has been implemented by Tonova et al. [17] — a method to reconstruct a general refractive-index profile with the use of the Newton–Kantorovitch algorithm on ellipsometric data measured at multiple angles of incidence.

An important issue with measuring the gradient refractive-index profile is that there is no reliable method able to set the true profile. Therefore, the discussion on the precision of reconstruction, beside the use of synthetic data [17], becomes problematic. In all the listed EMA-based articles, the precision of the attained gradient refractive-index model was not discussed. Hence, it remains unclear what is the actual precision attainable by using the commonly used optical characterization of a gradient thin film.

In this paper, we provide a detailed experimental study of optical characterization of an arbitrary gradient refractive index and we particularly focus on the precision of the gradient shape reconstruction. Namely, we employed DIBS-deposited SiO_xN_y layers, which were characterized with a broad set of methods: SE measurements and spectrophotometry measured at multiple incident angles. From the characterization of individual homogeneous thin films with a distinct oxygen and nitrogen stoichiometry, we attained an initial estimate of a refractive-index profile. Then, we used the same parameters with a varying stoichiometry to deposit a gradient thin layer and we measured its optical response.

The goal of our work was to alter the expected gradient profile to attain the best agreement between the experimental and the calculated optical response. We focused on the sensitivity of the agreement towards a variation in the profile offset, an addition or a subtraction of a quadratic function, or a random subtle modification of the initial model. While the controlled modification of the gradient refractive-index profile might suggest that the profile can be determined with a very high precision, we demonstrate that the experimental data can be reproduced by a broad set of profiles with the refractive index varying as much as 0.02 around the central value. Therefore, our work provides an insight into the precision which can be expected from refractive-index profile retrieval based on an optical characterization of a general gradient refractive-index thin film.

2. Experimental details

We deposited SiO_xN_y thin layers by DIBS apparatus described in [20]. DIBS is employed in this paper to enhance the control of stoichiometry and for qualities of deposited layers, i.e., density, adhesion, nucleation, etc. [21]. The primary ion source sputtered silicon from a target, and the assistant ion source generated reactions of oxygen and nitrogen with the sputtered silicon atoms to form SiO_xN_y. The beam voltage and beam current of the primary ion source were set to 600 V and 108 mA, respectively.

The assistant ion source parameters were set to 120 V for discharge voltage and 0.6 A for discharge current. Other parameters of the assistant ion source are representing gas flow. The flow of nitrogen was set to 49 sccm, and the flow of oxygen varied within 0 and 3 sccm.

We used plane-parallel N-BK7 as a substrate for all the depositions, except the deposition of homogeneous layers with the flow of oxygen of 2.5 and 3 sccm. For those, plane-parallel N-SF10 was used (i) because the deposited refractive index of the layers was too similar to the one of N-BK7, and (ii) because the lack of contrast would not allow reliable refractive-index retrieval.

Both the transmittance T and reflectance R spectra were measured within wavelengths of 380 and 980 nm by an EssenOptics Photon RT spectrometer. The measurements were carried out for the incident angles 4°, 8°, 20°, 30°, 40°, 50°, 60°, and 70°, where the angle of 4° was used only for the measurement of transmittance. All the spectra were measured for both the p- and s-polarization. The measurement step was set to 2 nm.

The ellipsometry measurements were carried out via Sentech SE850 with micro-spots. We measured visible range of wavelengths between 280 nm and 850 nm under the incident angle of 70°. The measurement step was set to 0.6 nm.

Due to good uniformity of the DIBS deposition, it was sufficient to take measurement at only one spot. The repeatability of the measurements was superb, so consequently all measurements were taken only once. Some statistical fluctuation of the measurements would have minimal impact on the final model.

3. Results and discussion

3.1. Homogeneous layers

The initial goal was to create a reliable model where the deposition parameters of SiO_xN_y are linked to a certain refractive-index dispersion curve.

We first deposited a set of samples of layers with a homogeneous refractive index where each sample had different stoichiometry of SiO_xN_y. In other words, we deposited a standard thin film for each sample featuring step-like refractive-index changes over interfaces.

In order to describe optical response of the optical coating, we applied a transfer-matrix approach described in detail in [22]. The method allows us to calculate the optical response (T, R and SE spectra at several incident angles), provided that we know the complex refractive index of a layer n_L, the substrate and incident medium together with the layer thickness. It is worth noting that the listed measurements represent the complete linear optical response of the sample. In order to reproduce the experimental data, we correct the transmittance and reflectance curve for a reflection from the uncoated (backside) substrate surface. The multiple reflections from the substrate backside were neglected.

In the description of the spectral shape of the optical characteristics for incident angle θ and wavelengths λ, we used the Tauc–Lorentz model of the refractive index [23]. This model is commonly used for wide-band gap dielectric materials. In our studies, we used two oscillators where one oscillator dominated and the second one accounted for a minor correction (1% of the amplitude). Parameters of the model were fitted by using a complete dataset acquired for a homogeneous layer of SiO_xN_y. The fittings included all the T, R, Ψ and Δ curves, and all of them optimized the model parameters with respect to the merit function

$$f_{\text{mer}} = \eta_T \sqrt{\sum_{\theta,\lambda} (\tilde{T}_{\theta\lambda} - T_{\theta\lambda})^2} + \eta_R \sqrt{\sum_{\theta,\lambda} (\tilde{R}_{\theta\lambda} - R_{\theta\lambda})^2} + \eta_\Delta \sqrt{\sum_{\theta,\lambda} (\tilde{\Delta}_{\theta\lambda} - \Delta_{\theta\lambda})^2} + \eta_\Psi \sqrt{\sum_{\theta,\lambda} (\tilde{\Psi}_{\theta\lambda} - \Psi_{\theta\lambda})^2}, \tag{1}$$

where the tilde symbol marks theoretical spectra made of the Tauc–Lorentz model, whereas the letters without tilde represent the measured spectra. The weight coefficients of transmittance (η_T), reflectance (η_R), function Ψ (η_Ψ) and function Δ (η_Δ) were set to 0.474, 0.474, 0.037 and 0.0046, respectively, to account for the different range and noise level of the T, R and ellipsometric functions. For the given weights, all the types of data contributed comparably to the resulting merit function values.

Figure 1a provides a comparison between the experimentally measured data (blue lines) and the model-based calculated curves (red lines) for selected incident angles and polarization. The applied Tauc–Lorentz model allowed us to achieve a refractive-index profile (see Fig. 1b) with a nearly ideal agreement. The fit was carried out for the whole set of deposited homogeneous layers, where the oxygen flow into the assistant ion source controlled the SiO_xN_y composition (see Table I for details). In close agreement with the previously reported values [7, 8, 19], we observe the decrease of the refractive index with the increasing oxygen flow rate. Namely, its values range from 2.02 (0 sccm, wavelength of 500 nm) up to 1.54 (3 sccm, wavelength of 500 nm).

By taking into account the gradual and smooth change of the refractive index with the oxygen ratio, we can fit the attained refractive-index dependence on the oxygen flow with a 4th order polynomial function (see Fig. 2a). From the deviation of the data points from the fit in Fig. 2a, we can estimate that our model leads to an error in the refractive index within ≈ 0.03. We reached the same precision when we employed this procedure on Si_3N_4 layers with various thicknesses ranging from 250 nm to 1500 nm. We ascribe this inaccuracy to the limitations posed by the double-oscillator Tauc–Lorenz model, which is an approximation of a more complex refractive-index dispersion curve of SiO_xN_y.

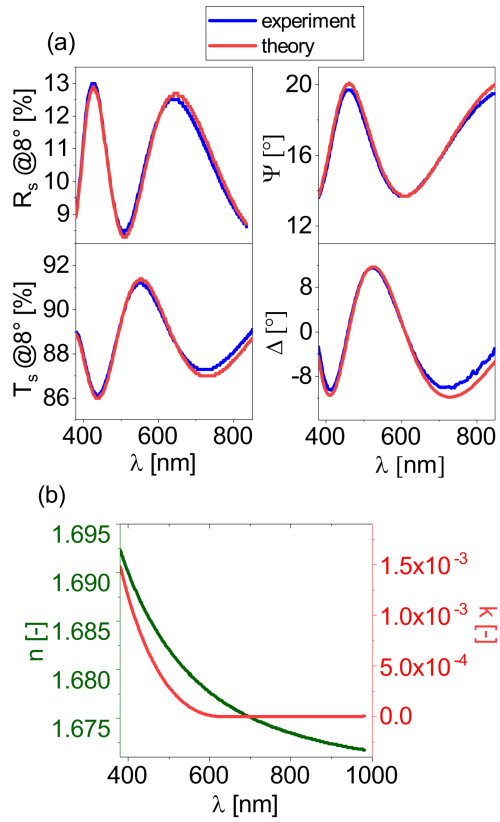

Fig. 1. Illustration of the homogeneous film characterization (oxygen flow 1.5 sccm): (a) Comparison of experimental (blue lines) and fitted theoretical spectra (red lines) of reflectance R, transmittance T (both s-polarization, incident angle 8°), and ellipsometric functions Δ and Ψ (incident angle 70°); (b) The attained refractive index (green line) and extinction coefficient (orange line) of the SiO_xN_y layer.

TABLE I

Retrieved refractive indices of the deposited homogeneous SiO_xN_y layers at 500 nm for a range of oxygen flows Q. Degree of the experiment–theory agreement is represented by merit function f_{mer} — see the main text for the details. The Tauc–Lorentz coefficients of the dominating first oscillator are presented.

Q [sccm]	d [nm]	n	k	f_{mer}	e_{inf}	E_g	A	E	C
0	295	2.026	2.70×10^{-3}	1.53	1.017	1.633	44.93	10.88	0.963
0.25	291	1.994	2.40×10^{-3}	1.21	0.917	1.527	45.63	11.62	0.805
0.5	299	1.857	5.10×10^{-4}	1.90	1.037	2.078	40.16	11.32	0.952
0.75	303	1.880	1.50×10^{-3}	1.37	0.711	1.704	49.70	13.65	1.080
1	327	1.746	5.70×10^{-4}	1.63	1.171	1.878	34.56	13.99	1.001
1.5	329	1.682	4.80×10^{-6}	0.87	1.413	2.554	28.51	13.09	1.022
2	346	1.610	1.20×10^{-3}	1.44	0.946	1.509	27.89	13.91	0.920
2.5	352	1.565	6.60×10^{-6}	1.25	0.942	2.573	32.30	14.81	0.819
3	357	1.543	1.10×10^{-4}	1.48	1.028	2.237	25.61	13.13	1.092

Although there was a slight irregularity of the rate, no dependence of the rate on oxygen flow was observed. It was evaluated based on the ratio between the deposited thickness of the homogeneous layers and their deposition time.

3.2. Gradient layers

The previous step allowed us to reliably trace changes of the refractive index for a varying oxygen flow in the assistant ion source. As a result, it was possible to attain a layer with a gradient refractive index by a slow variation in the oxygen supply. We deposited the gradient layer with a linear increase of the oxygen flow rate in time which leads to the decrease of the refractive index when z is increasing (see Fig. 2a). Note that $z = 0$ corresponds to the substrate surface.

The gradient layers were simulated as a set of 100 thin sublayers with a constant thickness by using the same approach as described in Sect. 3.1. The composition for a depth z can be derived from the deposition procedure, thus we can assign a refractive index $n(z_i)$ to the sublayers i with a known refractive-index model. The resulting refractive-index gradient $n(z)$ for each wavelength was determined based on spline interpolation of the $n(z_i)$ datapoints (see Fig. 2a, black line).

Optical response of the gradient layer was fitted by using the same merit function described in (1). However, the only fitting parameter was the layer thickness and the refractive index was fixed according to the estimated profile depicted in Fig. 2a. The resulting merit function of 1.17 was comparable to the ones attained for homogeneous layers. We obtained a very good agreement between the experimental data and the theoretical curves (see Fig. 2b). These results can be ascribed to the fact that the interpolation of the refractive index partly compensates for the errors in the models of the homogeneous layers.

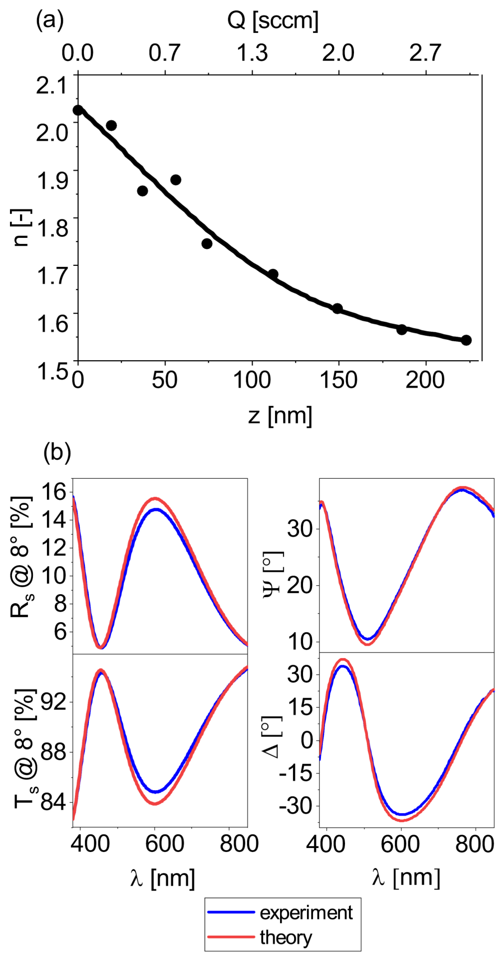

Fig. 2. (a) Gradient profile of the refractive-index at $\lambda = 500$ nm attained by 4th order polynomial fit (line) of the refractive-index attained for homogeneous films (circles); (b) Comparison of measured (blue lines) and simulated (red lines) optical response — reflectance, transmittance (both s-polarization, incident angle 8°), and ellipsometric functions Ψ and Δ (incident angle 70°).

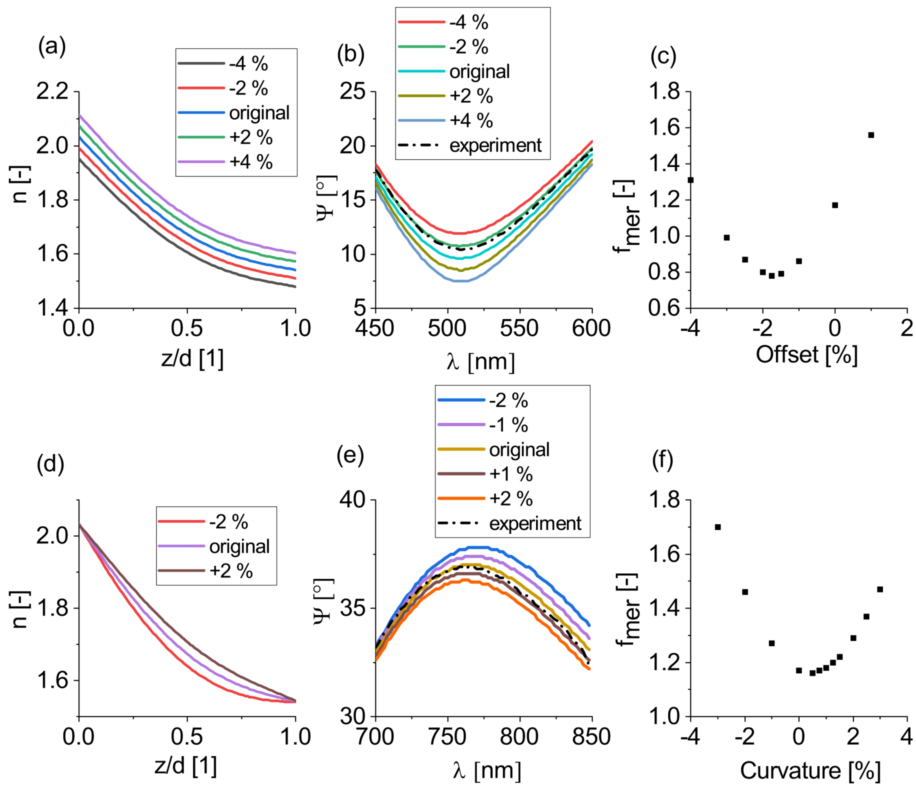

Fig. 3. Fit evaluation for systematic refractive-index variations by a variation of offset (a), (b), (c) and quadratic term addition (d), (e), (f). Examples of evaluated profiles with different parameters (a), (d). The sensitivity of Ψ function to the shape variation (b), (e). A change of the merit-function value with the shape variation (c), (f).

As a result, we were able to form a reliable initial model of the gradient layer together with its thickness determination. Nevertheless, the ultimate question of interest was to evaluate the precision of the estimated profile.

3.3. Systematical model variation

Using a free fit of all Tauc–Lorentz parameters for each of the nine concentrations (in total 81 parameters), is computationally prohibitive and the substantial number of parameters is likely not to converge to the best result. Therefore, we firstly studied the effect of two main expected imperfections, i.e., (i) the offset in the gradient refractive-index, (ii) the change in the overall shape of the gradient.

The offset in a refractive index is one of the problematic issues in material models, since the optical parameters can often be reproduced by using a higher or lower refractive index, which is compensated with a lower or higher layer thickness, respectively. We used the same refractive index as it was used in Fig. 2a, and we added an offset ranging from -5 to 5% of the original refractive index profile (see Fig. 3a). For each offset, we fitted the layer thickness and compared the merit functions of the samples (see Fig. 3c). We observe that the optimum offset was placed $\sim 2\%$ within the expected value. The effect of the offset on Ψ function around $\lambda = 500$ nm is illustrated in Fig. 3b.

Secondly, we have studied the effect of the change in the gradient shape. We altered the original gradient presented in Fig. 2a by adding a quadratic term — see Fig. 3d. Analogously to the previous case, we fitted the layer thickness in order to achieve the best merit function (see Fig. 3f).

We observed that the merit function values, i.e., the agreement between the experimental value and our gradient refractive-index model, are highly dependent on both offset and gradient profile bending. This suggests that, in principle, the gradient refractive index profile with a very high precision can be determined. Optimum offset can be located within 0.25% precision, implying the refractive-index precision reaching 0.005. We verified that the profile curve in arbitrary order of the parameters can be optimized, and thus we attained closely-lying curves. The one with the lowest merit function is depicted in Fig. 4 (dashed black line).

Therefore, the systematic fitting suggests that we can determine the refractive-index profile with a very high precision. However, as we will show in the next section, the systematical variation of the refractive-index model highly underestimates the actual profile determination inaccuracy.

3.4. Random model variation

We tested the actual precision of the optical characterization in a simulation. The refractive indices presented in Fig. 2a (dots) were altered by a set of random offsets with uniform distribution of ± 0.06. For each case, we fitted the refractive-index profile with the 4th order polynomial and carried out the fitting of the layer thickness. With 5,000 simulations, we attained an extensive set of gradient profiles with minute variations in their shape, which closely followed the original curve, and which in some cases featured a merit function value below the systematically optimized curve.

We selected the randomly modified profiles with the merit function below 0.8063. It corresponds to 10% higher value as compared to the best value attained via the systematical gradient variation (0.733) (see colored lines in Fig. 4). The curves with the lowest merit function differ from the systematically attained curve, and we evaluated their spread at several z points. The smallest spread is at $z = 200$ nm and $z = 225$ nm, where the values range from 1.559 to 1.577, and from 1.537 to 1.555, respectively. More generally, at most points the values differ by 0.02 from the mean value. The spread is the biggest at the edges of the layer. For instance, at $z = 0$, the refractive-index values vary from 1.969 to 2.043. However, this can be ascribed to the polynomial fitting of the data points, which is affected by the random change in the position of the last data point.

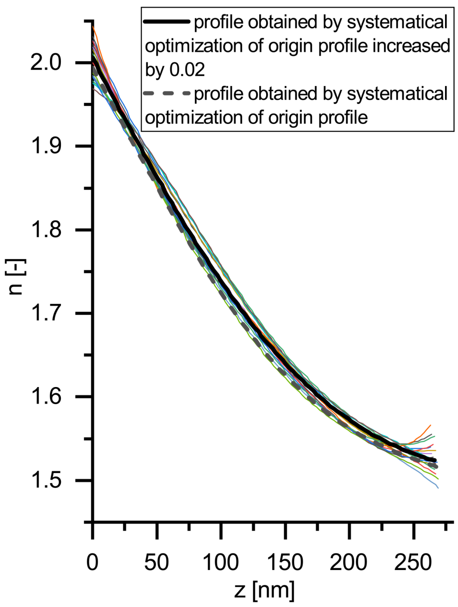

Fig. 4. Comparison of the refractive-index profiles attained by the random modification of refractive-index datapoints (colored lines) with the systematically optimized ones (black lines). Randomly modified curves were selected so that their fitting merit function was as lower compared to the systematic optimization (12 curves out of 5,000 modifications).

The comparison between the curve retrieved by the systematical variation (black dashed line in Fig. 4) with the randomly tested curves (colored lines in Fig. 4) raises a question why the systematical optimization did not converge to a curve located in the center of the best matching profiles of the random simulations. This is caused by the fact that even a minor change in the refractive-index profile highly affects the optimum offset and curvature. As an illustration, only by increasing the refractive index expected at the 1 sccm flow of oxygen by +0.02, we obtain, by the systematic optimization, a profile (solid black curve in Fig. 4), which lies in the center of the randomly optimized profile. In such a case, we also reached a significantly lower merit function value of 0.681. Therefore, the systematically varied parameters, despite featuring a sharp optimum value, do not reveal the actual profile precision.

4. Conclusions

We carried out a detailed study of optical characterization of SiO_xN_y graded thin films, where we aimed at extracting the refractive-index gradient shape based on the measurements of transmittance, reflectance and ellipsometry. We first attained an estimate of the refractive-index profile based on characterization of SiO_xN_y homogeneous thin films with varying stoichiometry. The estimated profile was varied in order to get the best agreement between the measured and simulated gradient thin film optical response.

We observed that the results might be seemingly very accurate when we scan one particular parameter, for instance, an offset of the gradient. Nevertheless, we can reproduce our experimental data with high precision by using a relatively broad range of gradients with the refractive index varying at most points of the profile by 0.02 from the mean value. We observe that the particular agreement highly varies with a subtle modification of the fixed points.

We propose that the precision of the measurement can be improved partly by forming a complex model, where we take into account multiple reflections on the thin layers and substrate. However, the solution of this problem highly depends on a particular experimental device, such as the dimension of the spectrometer's detector and light collection. Another prominent pathway is to propose a complex specific gradient shape, where the optical response will be more sensitive to the gradient actual shape.

Acknowledgments

We acknowledge the financial support of the Ministry of Education, Youth and Sports ("Partnership for Excellence in Superprecise Optics," Reg. No. CZ.02.1.01/0.0/0.0/16_026/0008390), and The Czech Academy of Sciences (Strategy AV21, programme 17). We also acknowledge the SGS project (SGS-2019-3054).

References

[1] O. Arnon, P. Baumeister, *Appl. Opt.* **19**, 1853 (1980).

[2] E. Welsch, D. Ristau, *Appl. Opt.* **34**, 7239 (1995).

[3] W.H. Southwell, *Appl. Opt.* **36**, 314, (1997).

[4] K. Luke, Y. Okawachi, M.R.E. Lamont, A.L. Gaeta, M. Lipson, *Opt. Lett.* **40**, 4823 (2015).

[5] L. Gao, F. Lemarchand, M. Lequime, *J. Eur. Opt. Soc.: Rapid Publ.* **8**, 13010 (2013).

[6] S. Callard, A. Gagnaire, J. Joseph, *J. Vac. Sci. Technol. A* **15**, 2088 (1997).

[7] P.G. Snyder, Yi-Ming Xiong, J.A. Woollam, G.A. Al-Jumaily, F.J. Gagliardi, *J. Vac. Sci. Technol. A* **10**, 1462 (1992).

[8] O.D. Volpian, A.I. Kuzmichev, Yu.A. Obod, *Inorg. Mater.: Appl. Res.* **6**, 234 (2015).

[9] M.F. Lambrinos, R. Valizadeh, J.S. Colligon, *Appl. Opt.* **35**, 3620 (1996).

[10] Huang-Lu Chen, Jin-Cherng Hsu, *Opt. Rev.* **16**, 226 (2009).

[11] H.-J. Erler, G. Reisse, C. Weissmantel, *Thin Solid Films* **65**, 233 (1980).

[12] J. Rivory, *Thin Solid Films* **313**, 333 (1998).

[13] V. Janicki, J. Sancho-Parramon, O. Stenzel, M. Lappschies, B. Gartz, C. Rickers, C. Polenzky, U. Richter, *Appl. Opt.* **46**, 6084 (2007).

[14] A.V. Tikhonravov, T.V. Amotchkina, M.K. Trubetskov, R.J. Francis, V. Janicki, J. Sancho-Parramon, H. Zorc, V. Pervak, *Appl. Opt.* **51**, 245 (2012).

[15] C.K. Carniglia, *J. Opt. Soc. Am. A* **7**, 848 (1990).

[16] G. Parjadis de Lariviére, J. M. Frigerio, J. Rivory, F. Abelés, *Appl. Opt.* **31**, 6056 (1992).

[17] D.A. Tonova, A.A. Konova, *Thin Solid Films* **397**, 17 (2001).

[18] D.A.G. Bruggeman, *Ann. Phys.* **416**, 636 (1935).

[19] Yi-Ming Xiong, P.G. Snyder, J.A. Woollam, G.A. Al-Jumaily, F.J. Gagliardi, E.R. Krosche, *Thin Solid Films* **206**, 248 (1991).

[20] K. Žídek, J. Hlubuček, P. Horodyská, J. Budasz, J. Václavík, *Thin Solid Films* **626**, 60 (2017).

[21] J.K. Hirvonen, *Mater. Sci. Rep.* **6**, 215 (1991).

[22] H. Angusmacleod, in: *Optical Thin Films and Coatings: From Materials to Applications*, Eds. A. Piegari, F. Flory, Woodhead Publishing, 2013, p. 3.

[23] G.E. Jellison, F.A. Modine, *Appl. Phys. Lett.* **69**, 371 (1996).